Electronic Supplementary Material (ESI) for RSC Advances.
This journal is © The Royal Society of Chemistry 2020

Supplementary Information

Novel method to identify group-specific non-catalytic pockets of human kinome for drug design

Huiwen Wang[1], Zeyu Guan[1], Jiadi Qiu[1], Ya Jia[1], Chen Zeng[1,2] and Yunjie Zhao[1*]

Author affiliation:

[1]Institute of Biophysics and Department of Physics, Central China Normal University, Wuhan 430079, China

[2]Department of Physics, The George Washington University, Washington DC 20052, USA

*Corresponding author

Yunjie Zhao Email: yjzhaowh@mail.ccnu.edu.cn

Description of Additional Supplementary Files

File Name: Dataset S1.xls

Description: The ATP interaction residues of kinase/ATP complex structures were identified using LigPlot.[1, 2] The first, second, and third columns represent the kinase group, kinase structure, and PDB ID. The hydrogen bonding and hydrophobic interaction residues are listed in the fourth and fifth columns. The Dataset S1.xls can be download from http://zhaoserver.com.cn/GSNC/index.html.

File Name: Dataset S2.xls.

Description: These are 42 residues in the ATP pocket of MAP2K2 kinase (PDB ID: 1S9I[3]). We re-numbered column positions of the 42 residues in the 168 kinase sequences alignment file from 1 to 42. Then we have counted the positions of all amino acid residues that interact with ATP to form hydrogen bonds from 15 complex structures. The hydrogen bonding residues mainly located at four positions. Two are charged residues located at position 11(K) and position 22(D/E). Another two residues located at positions 34 and 37 (mostly N/D). The Dataset S2.xls can be download from http://zhaoserver.com.cn/GSNC/index.html.

File Name: Dataset S3.xls.

Description: These are 42 residues in the ATP pocket of MAP2K2 kinase (PDB ID: 1S9I[3]). We re-numbered column positions of the 42 residues in the 168 kinase sequences alignment file from 1 to 42. Then we have counted the positions of all amino acid residues that interact with ATP to form hydrophobic interactions from 15 kinase/ATP complex structures. The hydrophobic interaction residues mainly located at eight positions. The residues in position 1 are mainly L or I, positions 2/4 are G, position 8 is V, position 9 is A, position 21 are M, F or T, position 23 are F, L or Y, and position 35 are L or M, respectively. The Dataset S3.xls can be download from http://zhaoserver.com.cn/GSNC/index.html.

File Name: Dataset S4.xlsx.

Description: The human kinome information extracted from Kinome Render. Some kinases (JAK1, JAK2, JAK3, MSK1, MSK2, RSK1, RSK2, RSK3, Tyk2, GCN2, RSK4, SPEG, Obscn) have two distinct catalytic domains (tagged with ~b). The Dataset S4.xls can be download from http://zhaoserver.com.cn/GSNC/index.html.

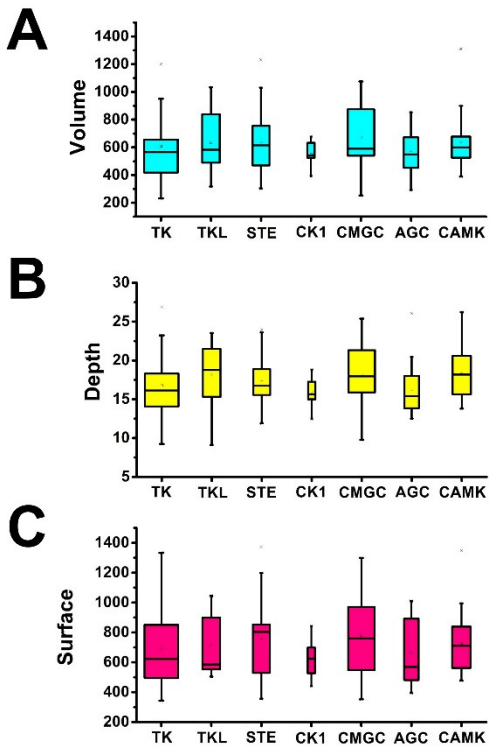

Fig. S1 Boxplots of the ATP pockets properties. (A) volume (Å^3), (B) depth (Å) and (C) surface (Å^2). The box width represents the number of ATP pockets contained in the respective groups.

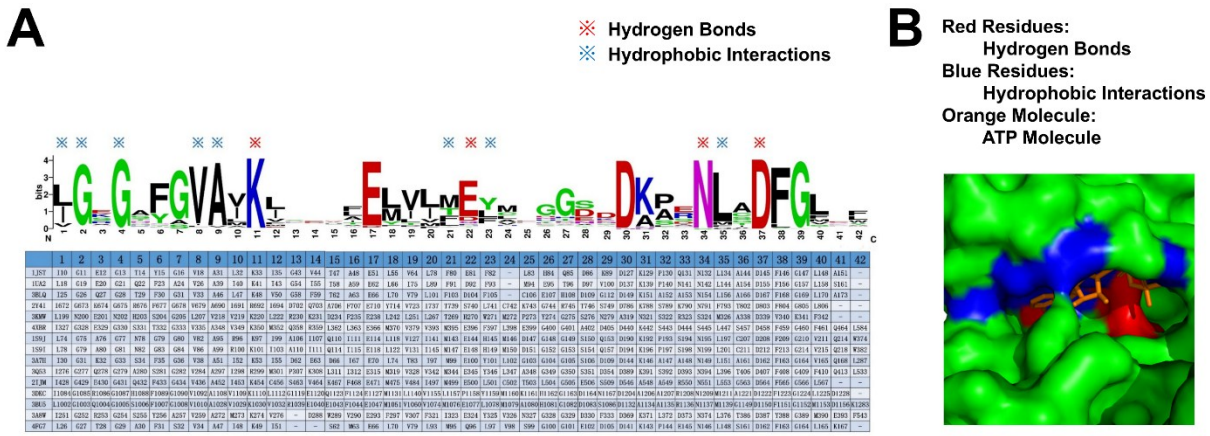

Fig. S2 The sequence evolutionary analysis of ATP pocket. (A) We have statistically analyzed the interactions between ATP molecule and pocket residues. The result shows four hydrogen bonds and eight hydrophobic interactions. (B) The surface representation of MAP2K2 kinase (PDB ID: 1S9I[3]). The ATP molecule, hydrogen bonding residues, hydrophobic interaction residues, and other MAP2K2 residues are colored in orange, red, blue, and green, respectively.

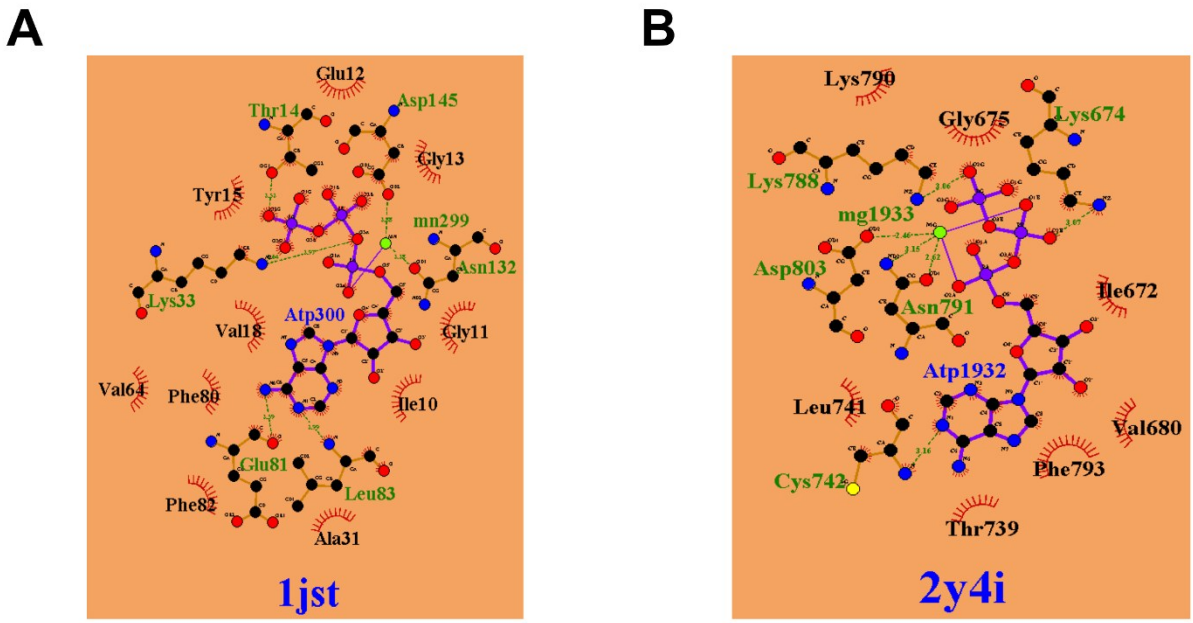

Fig. S3 The interactions between ATP molecule and pocket residues. (A) Asn132 and Asp145 of CDK2 (PDB ID: 1JST [4]) and (B) Asn791 and Asp803 of MAP2K1 (PDB ID: 2Y4I[5]) examples show that Asn and Asp residues in ATP pocket (positions 34 and 37 of Fig. 3A) form interactions via magnesium or manganese ions.

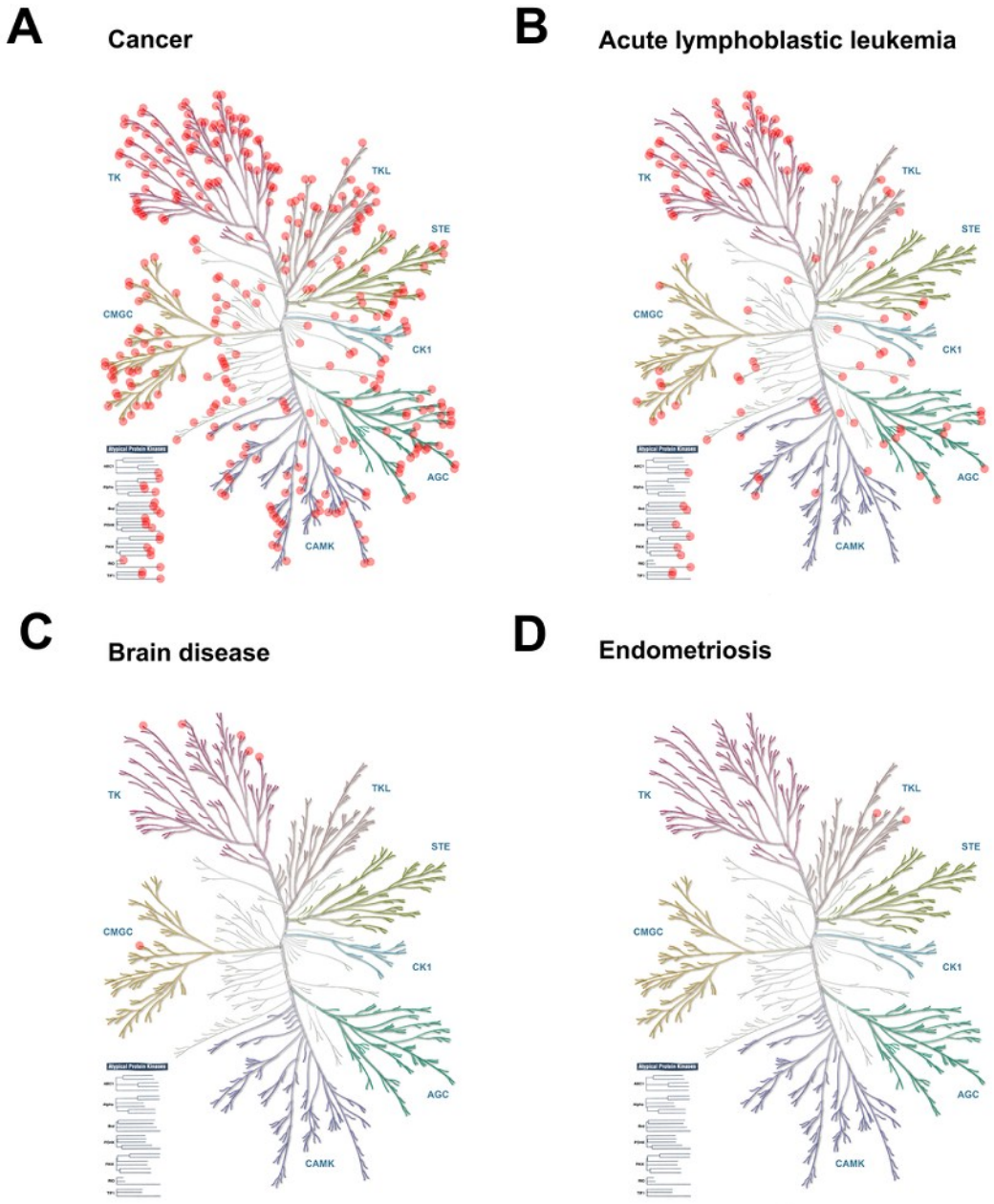

Fig. S4 The disease related human kinases of (A) cancer, (B) acute lymphoblastic leukemia, (C) brain disease, and (D) endometriosis. Cancer and acute lymphoblastic leukemia are related to almost all kinases. Brain disease and endometriosis are related to some specific kinase groups.

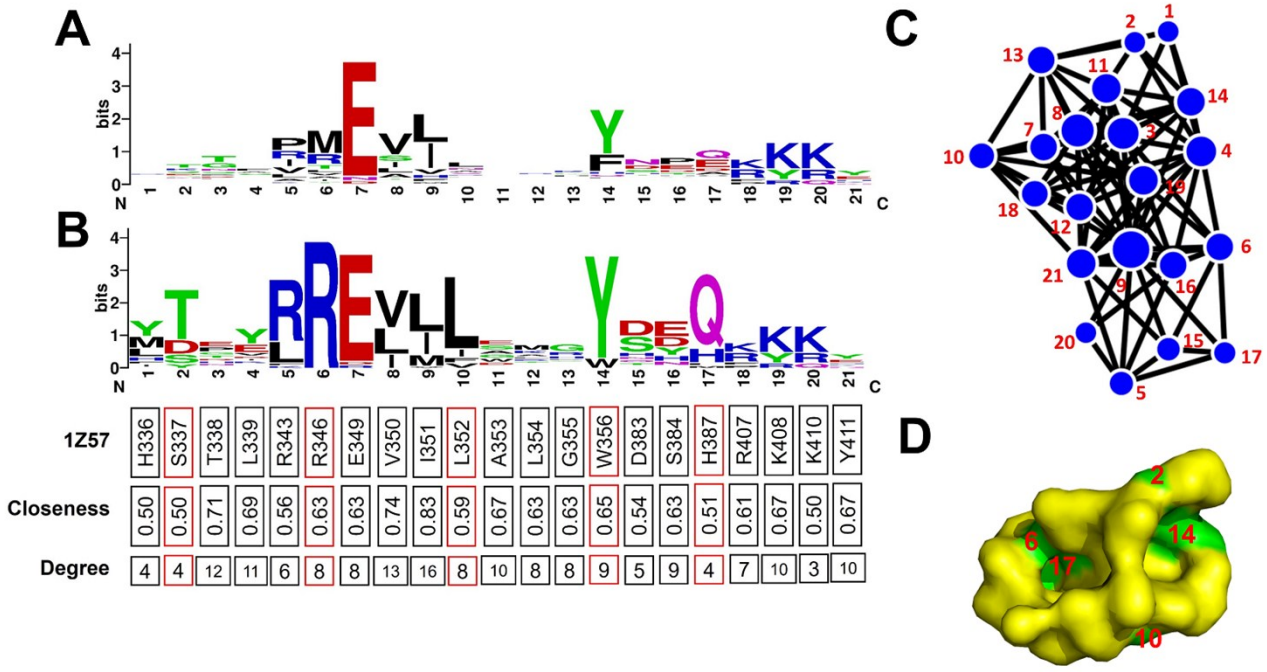

Fig. S5 The sequence variation analysis of p2 pocket from CLK1 kinase (PDB ID: 1Z57[6]) in the CMGC group. The differences between (A) kinome level and (B) CMGC group level shows specificity. The (C) network representative and (D) surface model of the p2 pocket indicate that the five residues (Ser337, Arg346, Ile352, Trp356 and His387 on position 2, 6, 10, 14 and 17, respectively) may be the crucial residues for p2 pocket from CLK1 kinase in CMGC group.

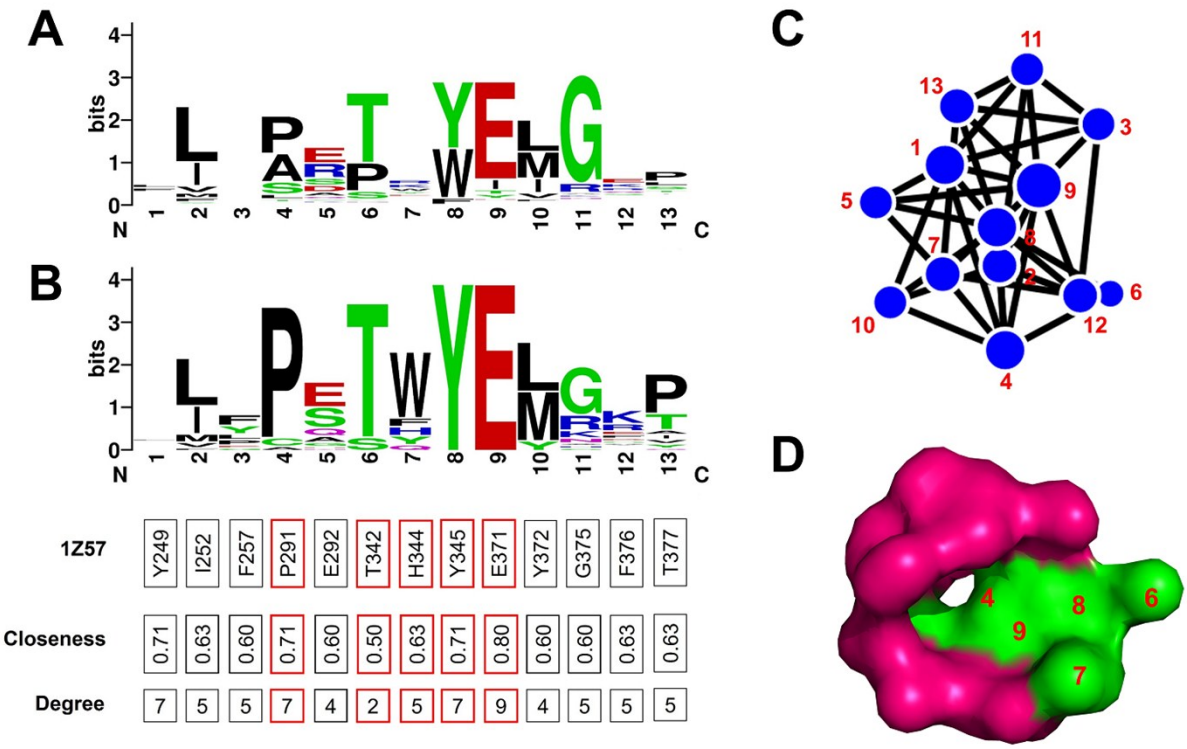

Fig. S6 The sequence variation analysis of p3 pocket from CLK1 kinase (PDB ID: 1Z57[6]) in the CMGC group. The differences between (A) kinome level and (B) CMGC group level show specificity. The (C) network representative and (D) surface model of the p3 pocket indicate that the five residues (Pro291, Thr342, His344, Tyr345 and Glu371 on position 4, 6, 7, 8 and 9, respectively) may be the crucial residues for p3 pocket from CLK1 kinase in CMGC group.

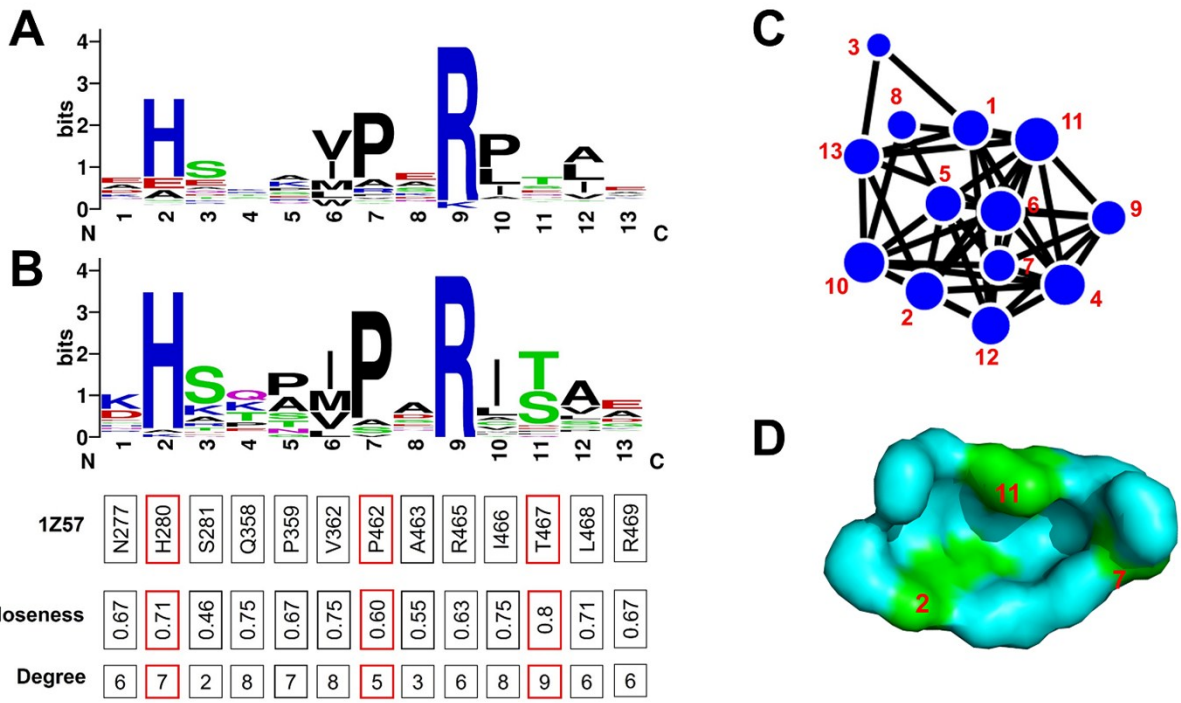

Fig. S7 The sequence variation analysis of p4 pocket from CLK1 kinase (PDB ID: 1Z57[6]) in the CMGC group. The differences between (A) kinome level and (B) CMGC group level show specificity. The (C) network representative and (D) surface model of the p4 pocket indicate that the three residues (His280, Pro462, and Thr467 on positions 2, 7 and 11, respectively) may be the crucial residues for p4 pocket from CLK1 kinase in CMGC group.

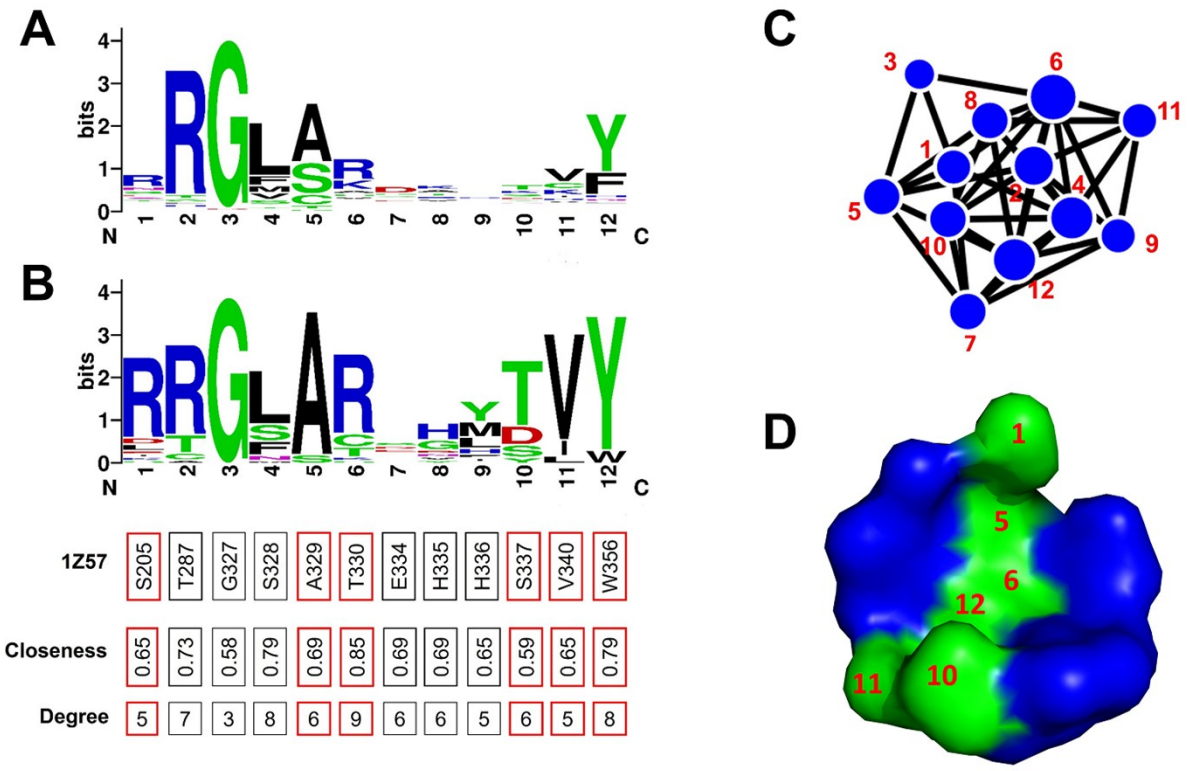

Fig. S8 The sequence variation analysis of p6 pocket from CLK1 kinase (PDB ID: 1Z57[6]) in the CMGC group. The differences between (A) kinome level and (B) CMGC group level show specificity. The (C) network representative and (D) surface model of the p6 pocket indicate that the six residues (Ser205, Ala329, Thr330, Ser337, Val340 and Trp356 on position 1, 5, 6, 10, 11 and 12, respectively) may be the crucial residues for p6 pocket from CLK1 kinase in CMGC group.

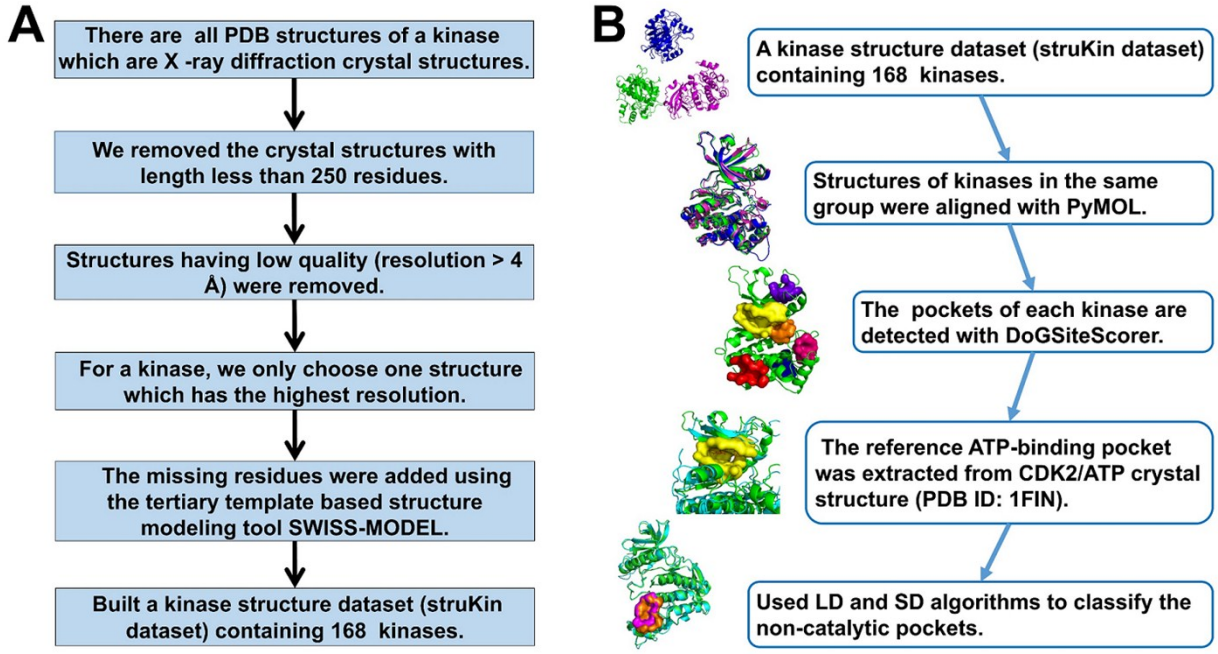

Fig. S9 The workflows of (A) non-redundant kinase structure dataset (struKin dataset) and (B) pocket detection and classification.

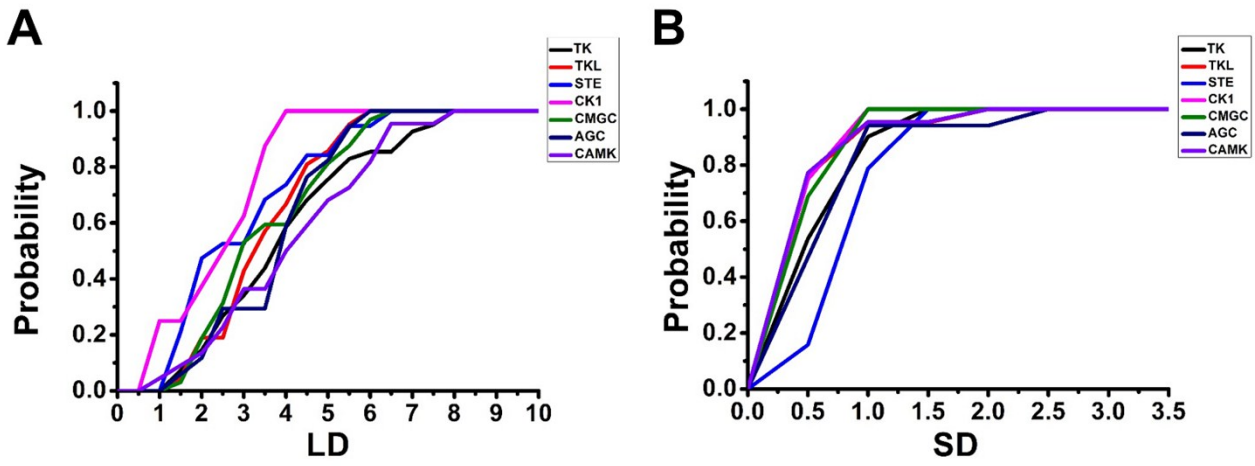

Fig. S10 The probabilities of ATP pocket shared in different groups for different location distance (LD) and shape distance (SD). (A) The result shows that the probabilities of ATP pocket shared in different groups remain unchanged if the LD is larger than 8 Å. (B) The result shows that the probabilities of ATP pocket shared in different groups remain unchanged if the SD is larger than 2.5 when LD=8 Å.

Table S1 The conservation analysis of ATP pockets, group shared non-catalytic (GSNC) pockets and non-GSNC pockets for different groups. The continuous conservation scores are divided into a discrete scale of 9 grades with grade 1 for the most variable positions while grade 9 the most conserved positions. The high average conservation scores suggest that ATP pockets are highly conserved. The reference kinases of CMGC, AGC, TKL, TK, CAMK, STE and CK1 groups are CLK1 (PDB ID: 1Z57[6]), Akt1 (PDB ID: 4GV1[7]), RIPK2 (PDB ID: 5J7B[8]), JAK1 (PDB ID: 3EYG[9]), CaMK1_alpha (PDB ID: 4FG8[10]), MST3 (PDB ID: 3A7I[11]) and CK1_alpha (PDB ID: 5FQD[12]), respectively.

Group	Reference Kinase	PDB ID	ATP pockets	GSNC pockets	Non-GSNC pockets
CMGC	CLK1	1Z57	p0 (7.3)	p2(5.7), p3(6.5), p4(5.5), p6(6.2), p7(5.1)	p1(4.3), p5(3.4), p8(4.3)
AGC	AKT1	4GV1	p0(7.6)	p1(5.8), p3(5.1), p4(6.8), p5(5.9), p8(4.7)	p2(3.8), p6(5.7), p7(5.6), p9(4.5), p10(4.6), p11(3.7), p12(6.3), p13(5.6), p14(5.2)
TKL	PIPK2	5J7B	p0(7.2)	p1(6.7), p3(5.9), p5(4.7)	P2(5.2), p4(5.5), p6(3.9), p7(4.7), p8(4.9), p9(5.0), p10(4.6), p11(6.0)
TK	JAK1	3EYG	p0(7.2)	p1(6.6), p2(8.4), p3(3.9), p6(5.9), p8(6.0)	p4(4.9), p5(3.1), p7(4.9), p9(4.5)
CAMK	CAMK1α	4FG8	p0(7.2)	p1(6.4), p2(6.7), p3(2.8)	p4(4.3), p5(6.6), p6(6.2), p7(5.7), p8(4.9), p9(3.1), p10(5.3), p11(4.9)
STE	MST3	3A7I	p0(7.5)	p5(4.7), p9(0.375)	p1(4.9), p2(4.9), p3(5.4), p4(5.6), p6(3.5), p7(4.9), p8(6.6), p10(4.4), p11(4.1), p12(8.3), p13(2.7)
CK1	CK1α	5FQD	p0(7.4)	p1(8.2), p2(5.8), p3(5.0), p6(3.4), p7(7.1), p12(6.5)	p4(4.2), p5(3.0), p8(5.5), p9(5.3), p10(7.6), p11(6.3)

Table S2 The identified 13 non-catalytic pockets from 6 human kinases (CDK2, CK2, Chk1, MAP14, MAP8 and c-Abl) by Ma et al.[13] The average volume, surface and depth size of these 13 non-catalytic pockets are 263.27(±110.58) $Å^3$, 414.64(±148.25) $Å^2$ and 10.23(±4.75) Å, respectively.

Kinase name	PDB ID	Pocket	Volume	Surface	Depth
CDK2	3PXZ[14]	P_4	462.78	615.87	14.16
Ck2α	3H30[15]	P_9	302.59	547.71	10.59
		P_10	305.54	359.25	13.98
		P_11	122.88	211.00	6.95
		P_12	186.62	310.60	13.08
Chk1	3JVR[16]	P_1_0	256.7	308.59	2.56
		P_2	213.7	400.95	12.88
MAP14	3NEW[17]	P_5	424.9	704.20	17.93
		P_6	249.09	442.57	9.97
		P_10	200.06	394.27	10.95
MAP8	3O2M[17]	P_7	114.03	221.98	8.59
		P_9	395.01	525.00	0.57
C-Abl	3PYY[18]	P_3	188.61	348.32	10.77

Table S3 The druggability scores of the ATP pockets, group shared non-catalytic (GSNC) pockets and non-GSNC pockets in seven groups. The pocket druggability score ranges from 0 to 1. The higher score indicates the more likely druggable pocket. The reference kinases of CMGC, AGC, TKL, TK, CAMK, STE and CK1 groups are CLK1 (PDB ID: 1Z57[6]), Akt1 (PDB ID: 4GV1[7]), RIPK2 (PDB ID: 5J7B[8]), JAK1 (PDB ID: 3EYG[9]), CaMK1_alpha (PDB ID: 4FG8[10]), MST3 (PDB ID: 3A7I[11]) and CK1_alpha (PDB ID: 5FQD[12]), respectively.

Group	Reference Kinase	PDB ID	ATP pocket	GSNC pocket's ranking	Non-GSNC pocket's ranking
CMGC	CLK1	1Z57	p0(0.808)	p2(0.663) > p7(0.450) > p4(0.441) > p3(0.435) > p6(0.241)	p1(0.822) > p5(0.258) > p8(0.256)
AGC	AKT1	4GV1	p0(0.513)	p8(0.488) > p4(0.487) > p5(0.477) > p3(0.449) > p1(0.109)	p2(0.799) > p6(0.382) > p10(0.306) > p7(0.295) > p9(0.276) > p14(0.242) > p13(0.231) > p11(0.224) > p12(0.151)
TKL	PIPK2	5J7B	p0(0.599)	p1(0.494) > p3(0.458) > p5(0.265)	P2(0.642) > p4(0.433) > p7(0.263) > p11(0.223) > p10(0.211) > p6(0.186) > p9(0.182) > p8(0.168)
TK	JAK1	3EYG	p0(0.560)	p6(0.396) > p8(0.255) > p1(0.188) > p3(0.162) > p2(0.119)	p4(0.692) > p5(0.475) > p7(0.263) > p9(0.181)
CAMK	CAMK1α	4FG8	p0(0.404)	p1(0.553) > p3(0.284) > p2(0.136)	p5(0.528) > p7(0.383) > p6(0.359) > p9(0.295) > p4(0.276) > p8(0.234) > p10(0.200) > p11(0.142)
STE	MST3	3A7I	p0(0.764)	P5(0.337) > p9(0.247)	p2(0.705) > p1(0.621) > p3(0.548) > p4(0.452) > p6(0.310) > p7(0.302) > p12(0.299) > p11(0.262) > p13(0.208) > p8(0.187) > p10(0.174)
CK1	CK1α	5FQD	p0(0.449)	p3(0.629) > p7(0.324) > p6(0.299) > p12(0.210) > p2(0.180) > p1(0.153)	p4(0.625) > p5(0.467) > p11(0.360) > p8(0.336) > p9(0.235) > p10(0.189)

Table S4 The allosteric kinase small molecules in the PDB database. The closeness values and predicted druggability scores of pockets are listed in the table.

Group	Pocket	Closeness	Druggability	Molecule
CMGC	GSNCp2	0.321	0.663	46A(3O2M[17]),
	GSNCp3	0.371	0.435	
	GSNCp4	0.339	0.441	
	GSNCp6	0.339	0.241	
	GSNCp7	0.320	0.450	3NE(3NEW[17]), 8OW(5N63[19]), 8OH(5N64[19]), 8ON(5N67[19]), 8OK(5N68[19]), O09(4E6A[20]), O08(4E6C[20]), O0A(4E8A[20]).
	Non-GSNCp1	0.333	0.822	NAN
	Non-GSNCp5	0.272	0.258	NAN
	Non-GSNCp8	0.290	0.256	NAN
AGC	GSNCp1	0.371	0.109	NAN
	GSNCp3	0.313	0.449	NAN
	GSNCp4	0.350	0.487	NAN
	GSNCp5	0.367	0.477	NAN
	GSNCp8	0.331	0.488	NAN
	Non-GSNCp2	0.285	0.799	NAN
	Non-GSNCp6	0.308	0.382	NAN
	Non-GSNCp7	0.347	0.295	NAN
	Non-GSNCp9	0.296	0.276	NAN
	Non-GSNCp10	0.310	0.306	NAN
	Non-GSNCp11	0.299	0.224	NAN
	Non-GSNCp12	0.363	0.151	NAN
	Non-GSNCp13	0.360	0.231	IQO(3O96[21]), 0R4(4EJN[22]), 6S1(5KCV[23])
	Non-GSNCp14	0.307	0.242	NAN
TKL	GSNCp1	0.368	0.494	NAN
	GSNCp3	0.356	0.458	NAN
	GSNCp5	0.325	0.265	NAN
	Non-GSNCp2	0.322	0.642	NAN
	Non-GSNCp4	0.343	0.433	NAN
	Non-GSNCp6	0.291	0.186	NAN
	Non-GSNCp7	0.346	0.263	NAN
	Non-GSNCp8	0.351	0.168	NAN
	Non-GSNCp9	0.325	0.182	NAN
	Non-GSNCp10	0.335	0.211	NAN
	Non-GSNCp11	0.350	0.223	NAN
TK	GSNCp1	0.370	0.188	NAN
	GSNCp2	0.408	0.119	0O7(4EBV[24]), OPE(4EBW[24])
	GSNCp3	0.324	0.162	NAN
	GSNCp6	0.369	0.396	1YZ(4M12[25]), 1E0(4M13[25])

	GSNCp8	0.356	0.255	NAN
	Non-GSNCp4	0.343	0.692	NAN
	Non-GSNCp5	0.275	0.475	NAN
	Non-GSNCp7	0.319	0.263	NAN
	Non-GSNCp9	0.315	0.181	NAN
CAMK	GSNCp1	0.346	0.553	NAN
	GSNCp2	0.357	0.136	NAN
	GSNCp3	0.325	0.284	NAN
	Non-GSNCp4	0.356	0.276	NAN
	Non-GSNCp5	0.375	0.528	NAN
	Non-GSNCp6	0.367	0.359	NAN
	Non-GSNCp7	0.371	0.383	NAN
	Non-GSNCp8	0.336	0.234	NAN
	Non-GSNCp9	0.328	0.295	NAN
	Non-GSNCp10	0.362	0.200	NAN
	Non-GSNCp11	0.298	0.142	NAN
STE	GSNCp5	0.326	0.337	NAN
	GSNCp9	0.375	0.247	NAN
	Non-GSNCp1	0.332	0.621	NAN
	Non-GSNCp2	0.301	0.705	NAN
	Non-GSNCp3	0.328	0.548	NAN
	Non-GSNCp4	0.367	0.452	NAN
	Non-GSNCp6	0.323	0.310	NAN
	Non-GSNCp7	0.347	0.302	NAN
	Non-GSNCp8	0.371	0.187	NAN
	Non-GSNCp10	0.324	0.174	NAN
	Non-GSNCp11	0.315	0.262	NAN
	Non-GSNCp12	0.395	0.299	NAN
	Non-GSNCp13	0.331	0.208	NAN
CK1	GSNCp1	0.386	0.153	NAN
	GSNCp2	0.347	0.180	NAN
	GSNCp3	0.351	0.629	NAN
	GSNCp6	0.344	0.299	NAN
	GSNCp7	0.356	0.324	NAN
	GSNCp12	0.339	0.210	NAN
	Non-GSNCp4	0.353	0.625	NAN
	Non-GSNCp5	0.323	0.467	NAN
	Non-GSNCp8	0.349	0.336	NAN
	Non-GSNCp9	0.318	0.235	NAN
	Non-GSNCp10	0.391	0.189	NAN
	Non-GSNCp11	0.382	0.360	NAN

Table S5 The cluster analysis of the group shared non-catalytic (GSNC) pockets at kinome level using cutoff LD = 8 Å and SD =2.5. Finally, a total of 14 GSNC pockets (GSNCp1 to GSNCp14 pockets) were identified in the entire human kinome.

GSNCp1 pocket	CMGC	CK1	TK	TKL
GSNCp2 pocket	CMGC	TKL	AGC	
GSNCp3 pocket	CMGC	CK1	AGC	
GSNCp4 pocket	TK	CK1	CAMK	
GSNCp5 pocket	CMGC	AGC		
GSNCp6 pocket	TK	STE		
GSNCp7 pocket	TK	AGC		
GSNCp8 pocket	CMGC	TK		
GSNCp9 pocket	STE	CK1		
GSNCp10 pocket	AGC	CK1		
GSNCp11 pocket	CK1			
GSNCp12 pocket	TKL			
GSNCp13 pocket	CAMK			
GSNCp14 pocket	CAMK			

Table S6 The crucial residues for group shared non-catalytic (GSNC) pockets of CLK1 kinase (PDB ID: 1Z57[6]) in the CMGC group.

Pocket	Critical residues
p2	S337, R346, L352, W356, Q387
p3	P291, T342, H344, Y345, E371
p4	H280, P462, T467
p6	S205, A329, T330, S337, V340, W357
p7	W356, P462

Reference

1. A. C. Wallace, R. A. Laskowski and J. M. Thornton, *Protein Eng.*, 1995, **8**, 127-134.
2. R. A. Laskowski and M. B. Swindells, *J. Chem. Inf. Model.*, 2011, **51**, 2778-2786.
3. J. F. Ohren, H. Chen, A. Pavlovsky, C. Whitehead, E. Zhang, P. Kuffa, C. Yan, P. Mcconnell, C. Spessard and C. Banotai, *Nat. Struct. Mol. Biol.*, 2004, **11**, 1192-1197.
4. A. A. Russo, P. D. Jeffrey and N. P. Pavletich, *Nat. Struct. Biol.*, 1996, **3**, 696-700.
5. D. F. Brennan, A. C. Dar, N. T. Hertz, W. C. Chao, A. L. Burlingame, K. M. Shokat and D. Barford, *Nature*, 2011, **472**, 366-369.
6. A. N. Bullock, S. Das, J. E. Debreczeni, P. Rellos, O. Fedorov, F. H. Niesen, K. Guo, E. Papagrigoriou, A. L. Amos, S. Cho, B.E. Turk, G. Ghosh, and S. Knapp, *Structure*, 2009, **17**, 352-362.
7. M. Addie, P. Ballard, D. Buttar, C. Crafter, G. Currie, B. R. Davies, J. Debreczeni, H. Dry, P. Dudley and R. Greenwood, P. D. Johnson, J.G. Kettle, C. Lane, G. Lamont, A. Leach, R. W. Luke, J. Morris, D. Ogilvie, K. Page, M. Pass, S. Pearson, L. Ruston, *J. Med. Chem.*, 2013, **56**, 2059-2073.
8. P. A. Haile, B. J. Votta, R. W. Marquis, M. J. Bury, J. F. Mehlmann, S. R. Jr, A. K. Charnley, A. S. Lakdawala, M. A. Convery and D. B. Lipshutz, *J. Med. Chem.*, 2016, **59**, 4867-4880.
9. N. K. Williams, R. S. Bamert, O. Patel, C. Wang, P. M. Walden, A. F. Wilks, E. Fantino, J. Rossjohn, I. S. Lucet, *J. Mol. Biol.*, 2009, **387**, 219-232.
10. M. Zha, C. Zhong, Y. Ou, L. Han, J. Wang and J. Ding, *Plos One*, 2012, **7**, e44828.
11. T. P. Ko, W. Y. Jeng, C. I. Liu, M. D. Lai, C. L. Wu, W. J. Chang, H. L. Shr, T. J. Lu and A. H. J. Wang, *Acta Crystallogr. D*, 2010, **66**, 145-154.
12. G. Petzold, E. S. Fischer and N. H. Thomä, *Nature*, 2016, **532**, 127-130.
13. X. Ma, H. Meng and L. Lai, *J. Chem. Inf. Model.*, 2016, **56**, 1725-1733.
14. S. Betzi, R. Alam, M. Martin, D. J. Lubbers, H. Han, S. R. Jakkaraj, G. I. Georg and E. Schönbrunn, *Acs Chem. Biol.*, 2011, **6**, 492-501.
15. J. Raaf, E. Brunstein, O. G. Issinger and K. Niefind, *Chem. Biol.*, 2008, **15**, 111-117.
16. D. Vanderpool, T. O. Johnson, C. Ping, S. Bergqvist, G. Alton, S. Phonephaly, E. Rui, C. Luo, Y. L. Deng and S. Grant, *Biochemistry*, 2009, **48**, 9823-9830.
17. K. M. Comess, C. Sun, C. Abadzapatero, E. R. Goedken, R. J. Gum, D. W. Borhani, M. Argiriadi, D. R. Groebe, Y. Jia and J. E. Clampit, *Acs Chem. Biol.*, 2011, **6**, 234-244.
18. J. Yang, N. Campobasso, M. P. Biju, K., Fisher, X. Q. Pan, J. Cottom, S. Galbraith, T. Ho, H. Zhang, X. Hong, P. Ward, G. Hofmann, B. Siegfried, F. Zappacosta, Y. Washio, P. Cao, J. Qu, S. Bertrand, D. Y. Wang, M. S. Head, H. Li, S. Moores, Z. Lai, K. Johanson, G. Burton, C. Erickson-Miller, G. Simpson, P. Tummino, R. A. Copeland and A. Oliff, *Chem. Biol.*, 2011, **18**, 177-186.
19. M. Bührmann, B. M. Wiedemann, M. P. Müller, J. Hardick, M. Ecke and D. Rauh, *Plos One*, **12**, e0184627.
20. N. Tzarum, Y. Eisenberg-Domovich, J. J. Gills, P. A. Dennis and O. Livnah, *J. Mol. Biol.*, 2012, **424**, 339-353.
21. W.I. Wu, W. C. Voegtli, H. L. Sturgis, F. P. Dizon, G. P. Vigers and B. J. Brandhuber, *Plos one*, 2010, **5**, e12913.
22. M. A. Ashwell, J.M. Lapierre, C. Brassard, K. Bresciano, C. Bull, S. Cornell-Kennon, S. Eathiraj, D. S. France, T. Hall and J. Hill, *J. Med. Chem.*, 2012, **55**, 5291-5310.
23. J.M. Lapierre, S. Eathiraj, D. Vensel, Y. Liu, C. O. Bull, S. Cornell-Kennon, S. Iimura, E. W. Kelleher, D. E. Kizer and S. Koerner, *J. Med. Chem.*, 2016, **59**, 6455-6469.
24. M. Iwatani, H. Iwata, A. Okabe, R. J. Skene, N. Tomita, Y. Hayashi, Y. Aramaki, D. J. Hosfield, A. Hori, A. Baba and H. Miki, *Eur. J. Med. Chem.*, **61**, 49-60.
25. S. Han, R. M. Czerwinski, N. L. Caspers, D. C. Limburg, W. Ding, H. Wang, J. F. Ohren, F. Rajamohan, T. J. Mclellan, R. Unwalla, C. Choi, M. D. Parikh, N. Seth, J Edmonds, C. Phillips, S. Shakya, X. Li, V. Spaulding. S. Hughes. A. Cook, C. Robinson, J. P. Mathias, I. Navratilova, Q. G. Medley, D. R. Anderson. R. G. Kurumbail and A. Aulabaugh, *Biochem. J.*, **460**, 211-222.